Human shoulder development is adapted to obstetrical constraints

Mikaze Kawada[a,1], Masato Nakatsukasa[a], Takeshi Nishimura[b], Akihisa Kaneko[b], Naomichi Ogihara[c], Shigehito Yamada[d], Walter Coudyzer[e], Christoph P. E. Zollikofer[f], Marcia S. Ponce de León[g], and Naoki Morimoto[a,1]

In humans, obstetrical difficulties arise from the large head and broad shoulders of the neonate relative to the maternal birth canal. Various characteristics of human cranial development, such as the relatively small head of neonates compared with adults and the delayed fusion of the metopic suture, have been suggested to reflect developmental adaptations to obstetrical constraints. On the other hand, it remains unknown whether the shoulders of humans also exhibit developmental features reflecting obstetrical adaptation. Here we address this question by tracking the development of shoulder width from fetal to adult stages in humans, chimpanzees, and Japanese macaques. Compared with nonhuman primates, shoulder development in humans follows a different trajectory, exhibiting reduced growth relative to trunk length before birth and enhanced growth after birth. This indicates that the perinatal developmental characteristics of the shoulders likely evolved to ease obstetrical difficulties such as shoulder dystocia in humans.

obstetrical dilemma | shoulder dystocia | ontogenetic allometry | childbirth

Childbirth is frequently a difficult task for humans compared with other large mammals. The obstetrical difficulties of humans result from a combination of a superoinferiorly short and anteroposteriorly deep pelvis of the mother and a large head and broad shoulders of the neonate. Obstetrical difficulties should, in principle, be eased by expanding the birth canal-related dimensions in the pelvis, especially the sacro–acetabular and biacetabular distances, and/or by reducing the critical cranial and shoulder dimensions of the fetus. However, the high prevalence of obstetrical difficulties in humans indicates that fetopelvic constraints remain unresolved. Various hypotheses have been proposed to explain this pattern. It has been suggested that more expansive pelvic dimensions could reduce the energetic efficiency of bipedal locomotion (1–5), could also be disadvantageous for bearing the weight of the visceral organs and the fetus during pregnancy (6–10), and may increase the risk of knee and ankle injuries due to increased stress along the mediolateral direction (11). The resulting obstetrical dilemma (12) has been hypothesized to persist in modern humans because of opposing and incompatible selective trends favoring large neonatal heads and narrow maternal birth canals (7, 10, 13, 14). Recently, the obstetrical dilemma hypothesis was challenged by various studies, indicating that locomotor cost is not increased by wider pelvic dimensions and proposing that fetal brain growth is constrained by the limits of maternal metabolism rather than by obstetrical constraints (15, 16).

It has been shown that obstetrical difficulties in humans are eased in various ways on both the maternal and neonatal sides. The first, which relates to mothers, consists of female-specific features of the pelvis, such as the laterally oriented ischiopubic region, flaring iliac blades, wide biacetabular distance, and a posteriorly projected sacrum (2, 17–20). A developmental study showed that these female-specific features are likely related to childbirth since they are expressed most strongly during the reproductive phase (21). In addition to the female-specific pelvic morphology, hormonal relaxation of the ligaments at the sacroiliac joints and pubic symphysis permits the bony pelvis to temporarily expand the birth canal during late pregnancy and childbirth (22–24). The second, which relates to both mothers and neonates, is cephalopelvic covariation (14, 25), which results in corresponding fetal head and maternal pelvic dimensions. The third, which relates to neonates, is the delayed ossification of the cranial vault during the fetal period. In humans, the fusion of the metopic suture is delayed compared with other primates. The metopic suture of humans is still unfused at birth, which is thought to permit the temporary deformation of the fetal head during childbirth (26–29). Additionally, the brain mass of the neonate relative to that of adults is smaller in humans (~30%) than in other primates such as chimpanzees (~40%) and macaques (~60%) (30). The perinatal head of humans thus shows various developmental features

likely associated with amelioration of the obstetrical dilemma and/or optimization of the perinatal metabolic demands of the mother and the fetus (15, 16).

How then about the broad shoulders of humans? The prevalence of shoulder dystocia, namely the arrest of fetal shoulders in the birth canal, is relatively high in humans (31, 32). In the contemporary human population, the frequency of shoulder dystocia increases linearly with neonatal body weight (33), and the risk of shoulder dystocia is notably high in cases of neonatal macrosomia (34–37). Shoulder dystocia can at times cause serious complications: On the fetal/neonatal side, it can cause asphyxia and/or brachial plexus injury that can lead to Erb's palsy (38–40); on the maternal side, it can lead to uterine rupture and/or excessive bleeding and, in the worst case, result in the death of neonates and/or mothers (41–43).

Here we investigate whether humans have evolved adaptive features in the shoulders to ease obstetrical difficulties, as is the case with the fetal head. The critical obstetrical dimension is fetal shoulder width, which varies to some extent with shoulder position, but is constrained by clavicular length. While clavicular growth from prenatal to postnatal stages has been studied in humans mainly as a measure to estimate the age at death (44–48), the obstetrical relevance of clavicular growth trajectories remains unknown. Specifically, we hypothesize that, in humans, the prenatal development of the shoulders is obstetrically constrained. To test this hypothesis, we investigate the developmental trajectory of the shoulders from fetal to adult stages in humans, chimpanzees, and Japanese macaques. These species show conspicuous differences in obstetrical constraints related to head and shoulder dimensions (Table 1), thus permitting the identification of childbirth-related developmental traits of the shoulders and head. In great apes, the broad shoulders do not complicate childbirth since neonatal size is small relative to maternal pelvic size, which stands in contrast to the large fetopelvic proportions in humans (19, 49). Macaques show a contrasting pattern to humans and great apes. They exhibit comparatively narrow shoulders, with the scapula located laterally on the trunk (50). Neonates are large relative to mothers, and the neonatal head dimensions are comparable to the maternal pelvic inlet dimensions, resulting in obstetrical constraints (1, 2, 19, 25, 30–33, 51).

Results

We measured cranial and postcranial skeletal dimensions in ontogenetic series of humans, chimpanzees, and Japanese macaques comprising fetal to adult stages. All measurements were taken on three-dimensional (3D) skeletal models derived from computed tomography (CT) data of cadaveric specimens (*Materials and Methods*, Fig. 1, and *SI Appendix*, Fig. S1 and Table S1). The shoulder girdle is a mobile structure, such that direct width measurements are influenced to some extent by its position and orientation relative to the trunk. We therefore use clavicular length as an additional static measure for shoulder width. The growth characteristics of the shoulders are compared with those of the head (obstetrically constrained) and those of the pelvis, humerus, and
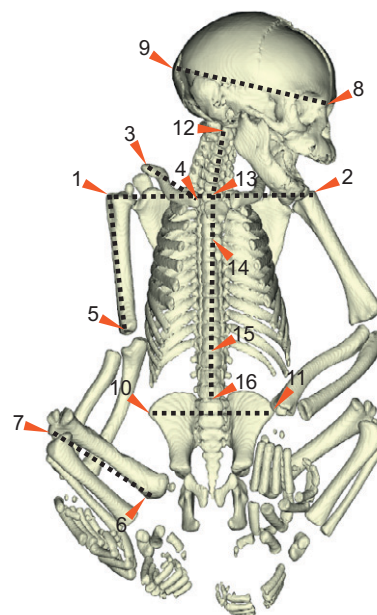

Fig. 1. Anatomical landmarks and linear measurements (shown on a neonatal chimpanzee). Red arrowheads indicate landmark locations. Dashed lines indicate linear measurements (shoulder width: 1 to 2; clavicular length: 3 to 4; humeral length: 1 to 5; femoral length: 6 to 7; cranial length: 8 to 9; pelvic width: 10 to 11; and trunk length: sum of the segments from 12 to 16). See *SI Appendix*, Table S3 for landmark definitions.

femur (obstetrically unconstrained). Trunk length (Fig. 1) serves as a reference for obstetrically unconstrained overall body growth. If the growth of the human shoulders is obstetrically constrained, we expect that its growth characteristics deviate from those of the obstetrically unconstrained postcranial skeletal elements. Growth trajectories were evaluated in two ways. First, we compared prenatal and postnatal ontogenetic allometric trajectories to characterize taxon-specific ontogenies and potential birth-related modifications (Fig. 2). Second, we focused on changes in growth rates around birth to further investigate potential obstetrical constraints during the transition from prenatal to postnatal growth characteristics (Figs. 3 and 4).

Figs. 2 and 3 and Table 2 show taxon-specific growth trajectories of the shoulders, cranium, pelvis, and long bones. In humans, the clavicular length exhibits negative ontogenetic allometry relative to the trunk before birth, and positive allometry after birth (Fig. 2A and Table 2; no statistical difference between males and females [*F* test and analysis of covariance; *SI Appendix*, Fig. S3 and Table S2]). In chimpanzees the clavicular length increases isometrically with trunk length, whereas in Japanese macaques the growth characteristics of the shoulders change from prenatal isometry to postnatal negative allometry (Fig. 2A and Table 2).

In humans, fetal cranial length and shoulder width grow in concordance (i.e., isometrically) and reach similar values around birth (Fig. 4), confirming the notion that head and shoulders are exposed to similar obstetrical constraints (51). After birth,

Table 1. Obstetrical conditions in humans, chimpanzees, and macaques

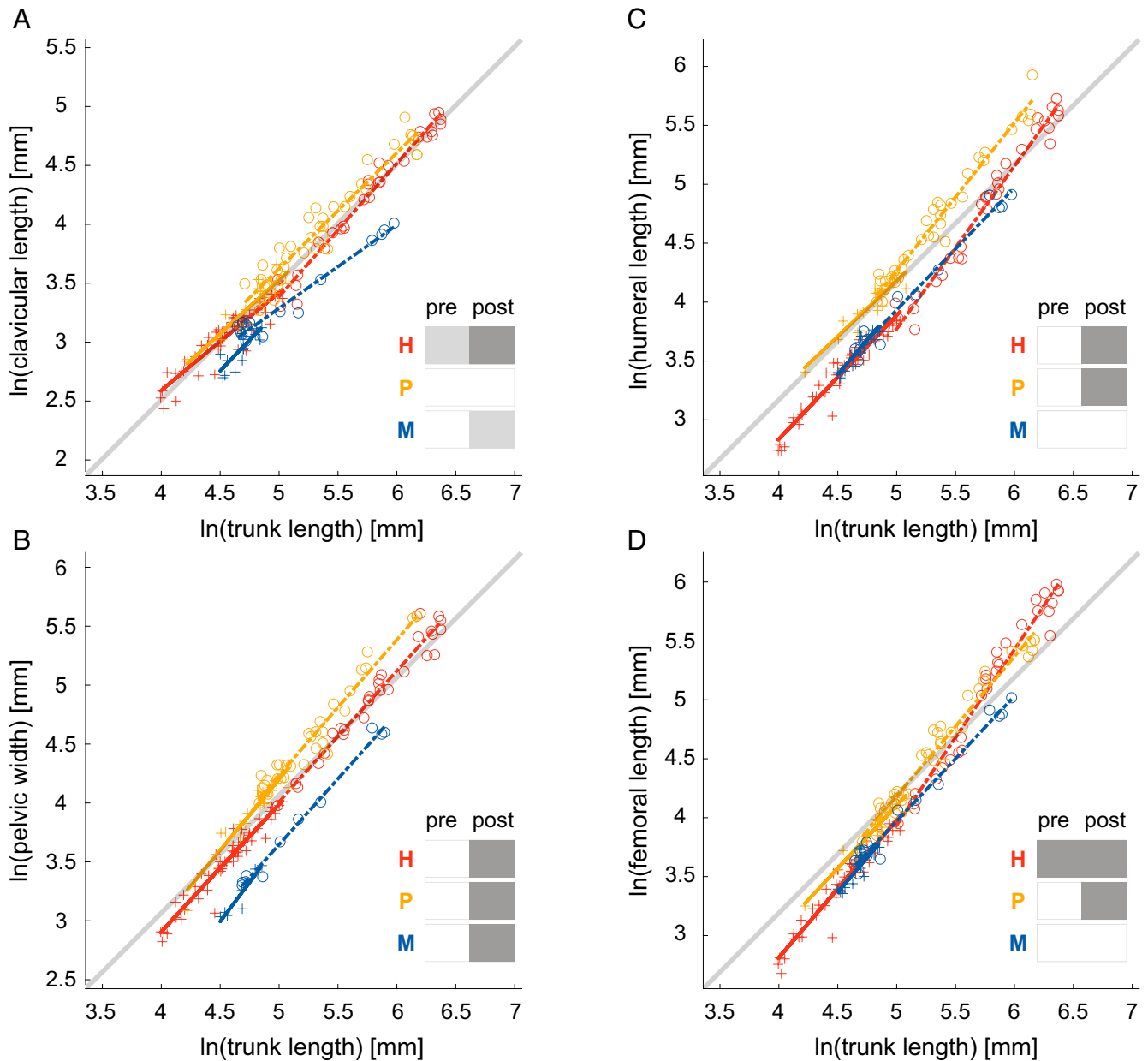| Species	Neonatal head size relative to birth canal	Shoulder width in adult	Neonatal shoulder width relative to birth canal (inlet)
Humans	Large	Wide	Wide
Chimpanzees	Small	Wide	Narrow
Macaques	Large	Narrow	Narrow

pnas.org

Fig. 2. Double-logarithmic plots of clavicular length (*A*), pelvic width (*B*), humeral length (*C*), and femoral length (*D*) versus trunk length. Crosses and circles indicate prenatal (pre) and postnatal (post) specimens, respectively (red: humans [H]; yellow: chimpanzees [P]; blue: Japanese macaques [M]). Least-squares regressions for prenatal and postnatal periods are shown as solid and dashed lines, respectively. Gray solid lines indicate isometric growth (slope = 1). Diagrams (*Lower Right*) in each plot show ontogenetic allometric characteristics (dark gray/light gray: positive/negative allometry; white: isometry). Only the human clavicle exhibits prenatal negative and postnatal positive allometric growth characteristics. See also Table 2.

cranial length grows at a lower rate than shoulder width, resulting in a negative allometric relationship that reflects reduced brain growth rate (Fig. 4). In chimpanzees and Japanese macaques, cranial length grows at lower rates than shoulder dimensions already before birth (Fig. 4).

In all the taxa studied here, the pelvis grows isometrically relative to the trunk during the prenatal period, and it shows positive allometry during the postnatal period (Figs. 2*B* and 3*B* and Table 2). The humerus grows isometrically relative to the trunk during the prenatal period in all the taxa studied here (Fig. 2*C* and Table 2). During the postnatal period, it grows with positive allometry in humans and chimpanzees, while it continues along an isometric trajectory in Japanese macaques (Fig. 2*C* and Table 2). The human femur grows with moderate positive allometry relative to the trunk during the prenatal period, and

with marked positive allometry during the postnatal period, reflecting high lower-limb extension rates resulting in the characteristic adult human body proportions (Fig. 2*D* and Table 2). In chimpanzees, the femur shows isometric and moderate positive allometric growth during prenatal and postnatal periods, respectively (Fig. 2*D* and Table 2). In Japanese macaques, the femur shows isometric growth during both prenatal and postnatal periods (Fig. 2*D* and Table 2).

Fig. 3 shows growth trajectories of relative clavicular, pelvic, and skull dimensions as functions of trunk length. The human-specific pattern of prenatal negative and postnatal positive allometry of the shoulders becomes manifest as a marked decrease of growth rates before birth followed by an increase after birth (Fig. 3*A*). In humans, such a perinatal growth depression is found only in the clavicular length (Fig. 3*A*),
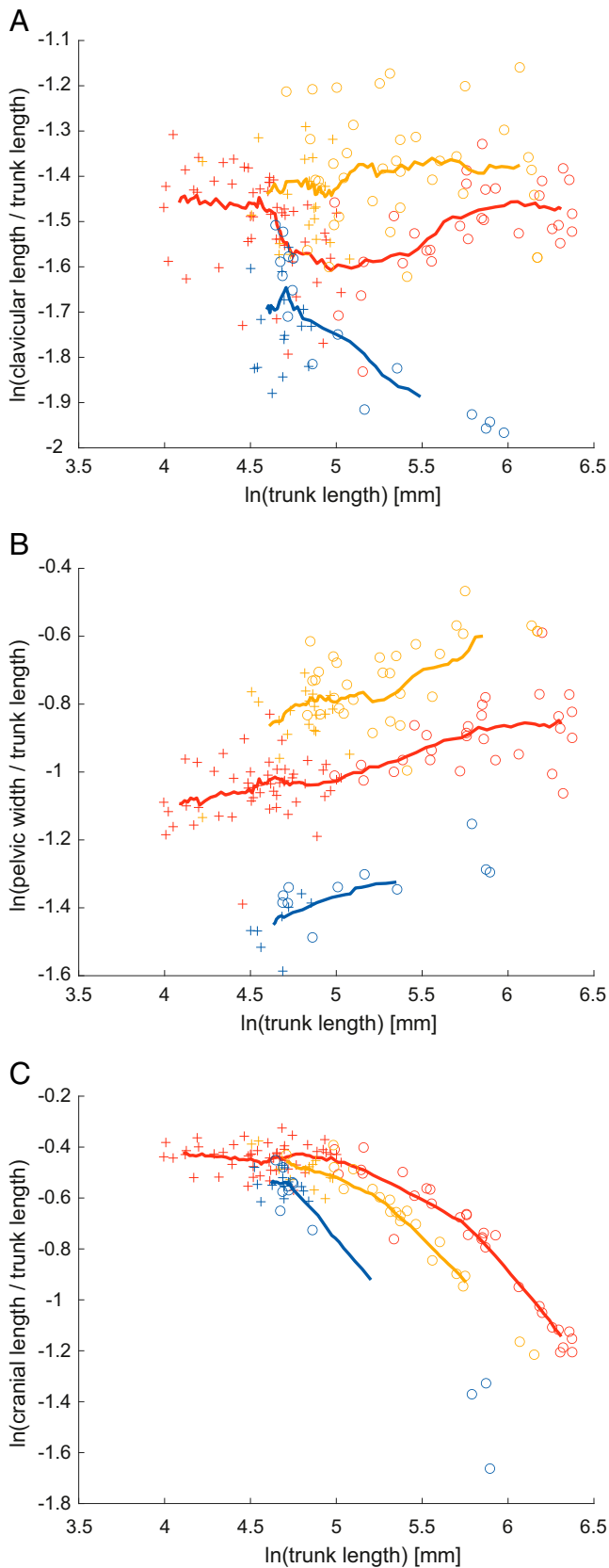
Fig. 3. Development of relative clavicular (*A*), pelvic (*B*), and cranial (*C*) dimensions (symbols and colors as in Fig. 2; moving-average trajectories). Human clavicular ontogeny is different from that in chimpanzees and Japanese macaques, showing a marked perinatal growth depression. In all species, pelvic width increases linearly relative to trunk length, while cranial length declines rapidly relative to trunk length after birth.

while relative pelvic width and relative cranial length increase and decrease, respectively (Fig. 3 *B* and *C*). The clavicular perinatal growth depression is not found in chimpanzees and Japanese macaques (Fig. 3*A*). In chimpanzees, the clavicular length is fairly constant relative to trunk length, while it declines after birth in Japanese macaques. In chimpanzees and Japanese macaques, growth trajectories of relative pelvic width and relative cranial length are largely similar, respectively, to those found in humans: Pelvic width shows a pattern of constant increase relative to trunk length throughout ontogeny (Fig. 3*B*), while cranial length shows a marked decline relative to trunk length after birth (Fig. 3*C*).

Discussion

Our results revealed a human-specific mode of shoulder growth, that is, a combination of prenatal negative and postnatal positive allometry (Fig. 2*A* and *SI Appendix*, Fig. S4) relative to trunk length and a growth depression around birth (Fig. 3*A*). These growth characteristics are exclusive to the shoulders, and not present in structures not involved in obstetrical complications such as the neonatal pelvis and long bones. Shoulder girdle and pelvic dimensions have been shown to covary in adult nonhuman primates, indicating correlated growth patterns (52). On the other hand, the relatively independent modes of human shoulder and pelvic ontogenies around birth (Fig. 3 *A* and *B*) likely indicate a higher degree of developmental modularity of the shoulder and pelvis in humans compared with nonhuman primates (53, 54) (also see ref. 55, showing reduced integration of limb development in humans and apes compared with monkeys). However, perinatal developmental modularity (as observed here) and adult morphological integration (as observed in ref. 52) do not contradict each other but rather represent different aspects of developmental coordination along the same ontogenetic trajectory. The perinatal growth depression of the human shoulder consists of a prenatal phase of growth deceleration followed by a postnatal phase of growth acceleration (Fig. 3*A*). This latter "catch-up" phase effectively reestablishes the correlation between pelvic, shoulder, and limb bone dimensions that is observed in adults (52, 56).

In any case, the human shoulder ontogeny cannot be explained by a generalized primate mode of postcranial ontogeny and likely represents a developmental feature that keeps the neonatal shoulders at the same width as the obstetrically relevant dimensions of the neonatal head (Fig. 4). In contrast to humans, neither chimpanzees nor Japanese macaques show a perinatal growth depression of the shoulders (Fig. 3*A*). The observed taxon-specific patterns of ontogenetic allometry (Figs. 3 and 4 and Table 2) are consistent with differences in obstetrical conditions and in adult shoulder width (Table 1): The broad shoulders of adult chimpanzees are achieved by maintaining the same growth rate (i.e., isometric growth relative to trunk length) throughout prenatal and postnatal ontogeny while those of humans are achieved by decelerated prenatal and accelerated postnatal development. Collectively, these results support the hypothesis that in humans the widening of the shoulder girdle during the prenatal period is constrained to ease obstetrical difficulties, while the postnatal growth catch-up yields wide adult shoulders (Figs. 2*A* and 3*A*).

If the perinatal growth depression of the human shoulders reflects an obstetrical adaptation, then why does the problem of shoulder dystocia persist? We hypothesize that human shoulder width faces a similar obstetrical dilemma as the head, namely an evolutionary conflict between selective pressures favoring
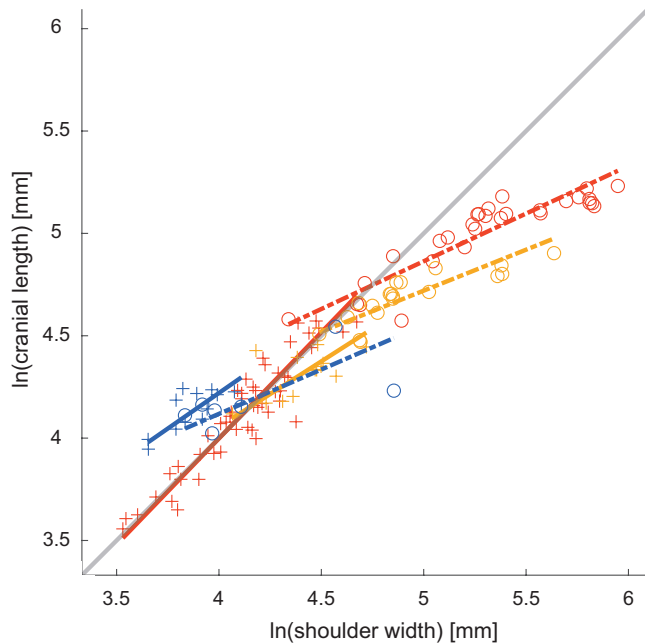
Fig. 4. Growth of cranial length relative to shoulder width (symbols and colors as in Fig. 2). In humans, shoulder width and cranial length tend to grow along the line of identity (shown in gray) until birth, resulting in similar obstetrically relevant dimensions. Only after birth does human shoulder width exceed cranial length (see *SI Appendix*, Table S4 for details).

large neonatal head (and shoulder) dimensions and pressures limiting birth canal dimensions, as proposed by the cliff-edge model for the evolution of fetopelvic proportions (13). Directional selection for wide neonatal shoulders could have several reasons. For humans, it has been argued that wide shoulders function to stabilize the trunk during bipedal locomotion and to facilitate high-speed throwing (57, 58). Another possible explanation could come from respiratory requirements. It is likely that shoulder width is functionally and developmentally linked to the size of the thorax. To initiate and sustain postnatal respiratory function, a certain size of the thorax is required. Thoracic growth disorder is one of the causes of thoracic insufficiency syndrome, defined as the inability of the thorax to support normal respiration or lung growth (59).

When, then, did the mode of shoulder development observed in modern humans emerge in the hominin lineage? DeSilva et al.

Table 2. Taxon-specific ontogenetic allometric patterns

Species	Structure	Prenatal	Postnatal
Humans	Clavicle	0.83 (0.05)*	1.13 (0.04)†
	Pelvis	1.08 (0.04)	1.11 (0.04)†
	Humerus	1.05 (0.04)	1.38 (0.05)†
	Femur	1.17 (0.05)†	1.49 (0.05)†
Chimpanzees	Clavicle	0.91 (0.11)	0.98 (0.05)
	Pelvis	1.21 (0.10)	1.15 (0.05)†
	Humerus	0.95 (0.08)	1.26 (0.04)†
	Femur	1.07 (0.08)	1.18 (0.04)†
Japanese macaques	Clavicle	1.05 (0.23)	0.71 (0.04)*
	Pelvis	1.13 (0.20)	1.12 (0.04)†
	Humerus	1.18 (0.17)	1.04 (0.05)
	Femur	1.18 (0.19)	1.06 (0.05)

Slopes of the regression lines and their SDs (in parentheses) of Fig. 2.
*Slopes that are statistically different from 1 ($P < 0.05$): negative allometry.
†Slopes that are statistically different from 1 ($P < 0.05$): positive allometry.

(60) proposed that *Australopithecus afarensis* could have had an elevated risk of shoulder dystocia, based on estimates of neonatal shoulder width. Following this proposition, we hypothesize that the prenatal restriction of shoulder growth evolved in the australopithecines. There is evidence that *Australopithecus africanus* exhibited a delayed fusion of the metopic suture (29) (but see ref. 61), which would indicate that obstetrical adaptations of the head and shoulders evolved in concert. These scenarios, however, remain to be tested with ontogenetic data of an expanded sample of primate species representing a wide range of shoulder widths (50). For example, gibbons also have wide shoulders, and there is a tight fit between neonatal head and maternal pelvic dimensions (19). Further studies will test the hypothesis that gibbons exhibit a similar perinatal mode of shoulder development as reported here for humans.

While the key obstetrical adaptation of the human shoulders consists of a perinatal growth rate depression, the obstetrical ontogenetic adaptation of the human head exhibits a different pattern. Prenatal brain growth in chimpanzees and macaques follows the typical trajectory of precocial mammals, where cerebral peak growth rates are reached long before birth (while in altricial mammals, they are reached after birth) (62, 63). Interestingly, brain growth in humans also follows the precocial pattern with a prenatal cerebral growth peak (63) but, compared with nonhuman primates, the peak is close to birth (62, 63). As an effect, human fetuses grow comparatively large heads, while growth rate reduction shortly before birth results in obstetrically compatible head dimensions. This pattern can be explained by each of the two main hypotheses on fetal cranial development: obstetrical constraints (12) and maternal metabolic constraints (16). Accordingly, the late prenatal timing of the human cerebral peak growth rate likely reflects a compromise between extended fetal brain growth on the one hand and maternal pelvic and metabolic constraints on the other.

In sum, we propose that human shoulder and head ontogenies both show evidence of obstetrical adaptations, but with different evolutionary foundations. The perinatal depression of shoulder growth rate is found only in humans (Figs. 2A and 3A) and likely evolved in the hominin lineage. In contrast, the prenatal decline of brain growth rate represents a primitive mode of ontogeny shared with other primates, which was pushed toward the limits imposed by obstetrical and/or maternal metabolic constraints. Together, these mechanisms result in a close match of the obstetrically relevant dimensions of the neonatal shoulders and skull (Fig. 4).

This study has explored the intricate effects of obstetrical constraints on human fetal development and neonatal body shape. Further studies are required to elucidate whether fetal–maternal obstetrical and metabolic constraints had even more pervasive effects on human ontogeny and developmental modularity and integration (56), and to what extent they represent evolutionary adaptations versus developmental plasticity.

Materials and Methods

Sample, Volumetric Data Acquisition, and Image Data Segmentation. The sample consists of whole-body specimens of humans (*Homo sapiens*; n = 81), chimpanzees (*Pan troglodytes*; n = 64), and Japanese macaques (*Macaca fuscata*; n = 31) ranging from late fetal to adult stages. See *SI Appendix*, Fig. S1 and Table S1 for details. The sample was collected from the following institutions: humans (fetal individuals): Congenital Anomaly Research Center at the Kyoto University Graduate School of Medicine (64); humans (prenatal and postnatal individuals): the digital autopsy database of University Hospitals Leuven; chimpanzees (prenatal and postnatal individuals): Department of Anthropology

at the University of Zurich (DAUZH) and Primate Research Institute of Kyoto University (KUPRI); and Japanese macaques: KUPRI. This study was approved by the ethics committee of the Faculty and Graduate School of Medicine of Kyoto University for the use of human fetal specimens (R0347). All the data from human individuals were anonymized prior to the present study.

The specimens were scanned using medical CT scanners (specimens of KUPRI: Canon Medical Systems; other specimens: Siemens or Philips). The CT scanning and image-reconstruction parameters are as follows: beam collimation 0.5 to 5.0 mm, slice reconstruction interval 0.2 to 1.5 mm, and reconstruction kernels ("bone" kernels; Canon, FC30/FC31; Siemens/Philips, B60s). Small specimens of DAUZH (length < 150 mm and diameter < 740 mm) were scanned using a micro-CT scanner (μCT80, Scanco Medical), and volume data were reconstructed at an isotropic voxel resolution of 75 μm.

Three-dimensional surfaces of the ossified structures were segmented from the CT volumetric data by setting a bone threshold and then applying the marching-cubes algorithm with the half-maximum threshold criterion, as implemented in Amira 2019.1 (Thermo Fisher Scientific).

Assessment of Developmental Stage. To compare the developmental patterns between prenatal and postnatal periods, we divided the entire sample into prenatal and postnatal subsamples. Since the age at death was unknown except for the anonymized human subsample, we used skeletal features to differentiate prenatal and postnatal individuals. For humans, we used the status of the tympanic ring as an indicator of developmental stage; fusion of the tympanic ring and squamous plate begins around the gestational age of 35 wk and is completed in most of the neonates (65). We categorized individuals with incomplete fusion of the tympanic ring and squamous plate as fetuses and those with complete tympanic rings as postnatal specimens. For chimpanzees and Japanese macaques, we used the status of the metopic suture as an indicator. The metopic suture closes often shortly after birth and is partially or completely fused before the eruption of the first deciduous tooth in most chimpanzees (29) and Japanese macaques; the first deciduous tooth erupts at the postnatal age of 1.5 mo in chimpanzees and 20 d in Japanese macaques, on average (66–68). We categorized chimpanzee and Japanese macaque specimens with a fused metopic suture as postnatal individuals.

Morphometric Data Acquisition and Analysis. To track skeletal growth, we took the following measurements on the virtual 3D models of the whole-body skeleton: cranial length, clavicular length, shoulder width, humeral and femoral length, pelvic width, and trunk length (Fig. 1). The shoulder width was measured as the linear distance between the most lateral points on the proximal epiphyseal lines of the left and right humeri (Fig. 1). Because the shoulder girdle is a mobile anatomical unit, direct measurements of its maximum width tend to depend on its postmortem position relative to the trunk. We therefore use the clavicular length as a dimension that constrains the shoulder width independent of shoulder position. *SI Appendix*, Fig. S2 shows a tight correlation between the shoulder width and clavicular length, such that the latter measurement serves as a proxy for the former. The clavicular length was measured as the linear distance between the center of the sternal and acromial articular facets (Fig. 1). The humeral and femoral lengths were measured as linear distances between the proximal and distal ends on epiphyseal lines (Fig. 1). The pelvic width was measured as the linear

(Euclidean) distance between the most lateral points of the right and left iliac blades (Fig. 1). The trunk length was measured as the sum of linear distances between the most anterosuperior points of the following segments: C1 (the first cervical vertebra) to T1 (the first thoracic vertebra), T1 to T5, T5 to L1 (the first lumbar vertebra), and L1 to the most anteroinferior point of the last lumbar vertebra (Fig. 1). All landmarks used in this study were set on the CT-based 3D surfaces representing the ossified skeletal structures (Fig. 1 and *SI Appendix*, Table S3). All linear distances were calculated as Euclidean distances between anatomical landmarks, using a MATLAB-based in-house program, ForMATit (MathWorks, version R2019b). See Fig. 1 and *SI Appendix*, Table S3 for definitions of landmarks.

Using trunk length as a proxy for obstetrically unconstrained body dimensions, we evaluated taxon-specific ontogenetic allometric trajectories of the clavicular length, pelvic width, humeral length, and femoral length (Figs. 2 and 3). Least-squares regressions were calculated for prenatal and postnatal periods on logarithmized dimensions (natural logarithm). We performed F tests to evaluate whether the slope a of the regression line differs significantly from 1 ($P < 0.05$). Slopes $a > 1$ and $a < 1$ indicate positive and negative ontogenetic allometric growth, respectively, whereas slopes that are not statistically different from 1 indicate isometric growth. We revealed further details of changes in relative skeletal growth rates along ontogenetic trajectories by plotting the log ratios of clavicular length, pelvic width, and cranial length to trunk length (Fig. 3). The resulting slopes $a' = a - 1$, which were drawn using the moving average, are positive/negative for positive/negative ontogenetic allometry, respectively, and zero for isometry. All the calculations were performed using MATLAB.

Data Availability. All study data are included in the article and/or *SI Appendix*.

Author affiliations: [a]Laboratory of Physical Anthropology, Graduate School of Science, Kyoto University, 606-8502 Kyoto, Japan; [b]Primate Research Institute, Kyoto University, 484-8506 Inuyama, Japan; [c]Department of Biological Sciences, Graduate School of Science, The University of Tokyo, Tokyo 113-0033, Japan; [d]Congenital Anomaly Research Center, Kyoto University Graduate School of Medicine, 606-8303 Kyoto, Japan; [e]Department of Radiology, University Hospitals, Katholieke Universiteit Leuven, 3000 Leuven, Belgium; [f]Anthropological Institute and Museum, University of Zurich, 8057 Zurich, Switzerland; and [g]Department of Informatics, University of Zurich, 8050 Zurich, Switzerland

1. K. Rosenberg, W. Trevathan, Birth, obstetrics and human evolution. *BJOG* **109**, 1199–1206 (2002).
2. K. R. Rosenberg, The evolution of modern human childbirth. *Am. J. Phys. Anthropol.* **35**, 89–124 (1992).
3. C. B. Ruff, Biomechanics of the hip and birth in early *Homo*. *Am. J. Phys. Anthropol.* **98**, 527–574 (1995).
4. R. G. Tague, C. O. Lovejoy, The obstetric pelvis of A.L. 288-1 (Lucy). *J. Hum. Evol.* **15**, 237–255 (1986).
5. A. B. Wittman, L. L. Wall, The evolutionary origins of obstructed labor: Bipedalism, encephalization, and the human obstetric dilemma. *Obstet. Gynecol. Surv.* **62**, 739–748 (2007).
6. E. H. M. Sze, N. Kohli, J. R. Miklos, T. Roat, M. M. Karram, Computed tomography comparison of bony pelvis dimensions between women with and without genital prolapse. *Obstet. Gynecol.* **93**, 229–232 (1999).
7. E. Stansfield, K. Kumar, P. Mitteroecker, N. D. S. Grunstra, Biomechanical trade-offs in the pelvic floor constrain the evolution of the human birth canal. *Proc. Natl. Acad. Sci. U.S.A.* **118**, e2022159118 (2021).
8. M. M. Abitbol, Evolution of the ischial spine and of the pelvic floor in the Hominoidea. *Am. J. Phys. Anthropol.* **75**, 53–67 (1988).
9. K. M. Brown, V. L. Handa, K. J. Macura, V. B. DeLeon, Three-dimensional shape differences in the bony pelves of women with pelvic floor disorders. *Int. Urogynecol. J. Pelvic Floor Dysfunct.* **24**, 431–439 (2013).
10. M. Pavlicev, R. Romero, P. Mitteroecker, Evolution of the human pelvis and obstructed labor: New explanations of an old obstetrical dilemma. *Am. J. Obstet. Gynecol.* **222**, 3–16 (2020).
11. E. Alentorn-Geli *et al.*, Prevention of non-contact anterior cruciate ligament injuries in soccer players. Part 1: Mechanisms of injury and underlying risk factors. *Knee Surg. Sports Traumatol. Arthrosc.* **17**, 705–729 (2009).
12. S. L. Washburn, Tools and human evolution. *Sci. Am.* **203**, 63–75 (1960).
13. P. Mitteroecker, S. M. Huttegger, B. Fischer, M. Pavlicev, Cliff-edge model of obstetric selection in humans. *Proc. Natl. Acad. Sci. U.S.A.* **113**, 14680–14685 (2016).
14. B. Fischer, P. Mitteroecker, Covariation between human pelvis shape, stature, and head size alleviates the obstetric dilemma. *Proc. Natl. Acad. Sci. U.S.A.* **112**, 5655–5660 (2015).
15. H. M. Dunsworth, There is no "obstetrical dilemma": Towards a braver medicine with fewer childbirth interventions. *Perspect. Biol. Med.* **61**, 249–263 (2018).
16. H. M. Dunsworth, A. G. Warrener, T. Deacon, P. T. Ellison, H. Pontzer, Metabolic hypothesis for human altriciality. *Proc. Natl. Acad. Sci. U.S.A.* **109**, 15212–15216 (2012).
17. H. Correia, S. Balseiro, M. De Areia, Sexual dimorphism in the human pelvis: Testing a new hypothesis. *Homo* **56**, 153–160 (2005).
18. E. A. Moffett, Dimorphism in the size and shape of the birth canal across anthropoid primates. *Anat. Rec. (Hoboken)* **300**, 870–889 (2017).
19. A. H. Schultz, Sex differences in the pelves of primates. *Am. J. Phys. Anthropol.* **7**, 401–423 (1949).
20. M. LaVelle, Natural selection and developmental sexual variation in the human pelvis. *Am. J. Phys. Anthropol.* **98**, 59–72 (1995).
21. A. Huseynov *et al.*, Developmental evidence for obstetric adaptation of the human female pelvis. *Proc. Natl. Acad. Sci. U.S.A.* **113**, 5227–5232 (2016).

22. M. K. Stoller, "The obstetric pelvis and mechanism of labor in nonhuman primates," PhD thesis, University of Chicago, Chicago, IL (1995).
23. N. M. Laudicina, M. Cartmill, Obstetric constraints in large-brained cebids and modern humans: A comparison of coping mechanisms. *Am. J. Phys. Anthropol.* **168**, 137 (2019).
24. K. Björklund, P. G. Lindgren, S. Bergström, U. Ulmsten, Sonographic assessment of symphyseal joint distention intra partum. *Acta Obstet. Gynecol. Scand.* **76**, 227–232 (1997).
25. M. Kawada, M. Nakatsukasa, T. Nishimura, A. Kaneko, N. Morimoto, Covariation of fetal skull and maternal pelvis during the perinatal period in rhesus macaques and evolution of childbirth in primates. *Proc. Natl. Acad. Sci. U.S.A.* **117**, 21251–21257 (2020).
26. O. Ami *et al.*, Three-dimensional magnetic resonance imaging of fetal head molding and brain shape changes during the second stage of labor. *PLoS One* **14**, e0215721 (2019).
27. S. R. K. Chopra, The cranial suture closure in monkeys. *Proc. Zool. Soc. Lond.* **128**, 67–112 (1957).
28. N. A. Beischer, E. V. Mackay, *Obstetrics and the Newborn: An Illustrated Textbook* (Saunders, 1986).
29. D. Falk, C. P. E. Zollikofer, N. Morimoto, M. S. Ponce de León, Metopic suture of Taung (*Australopithecus africanus*) and its implications for hominin brain evolution. *Proc. Natl. Acad. Sci. U.S.A.* **109**, 8467–8470 (2012).
30. J. M. DeSilva, J. J. Lesnik, Brain size at birth throughout human evolution: A new method for estimating neonatal brain size in hominins. *J. Hum. Evol.* **55**, 1064–1074 (2008).
31. E. A. Øverland, L. J. Vatten, A. Eskild, Risk of shoulder dystocia: Associations with parity and offspring birthweight. A population study of 1 914 544 deliveries. *Acta Obstet. Gynecol. Scand.* **91**, 483–488 (2012).
32. J. G. Ouzounian, R. B. Gherman, Shoulder dystocia: Are historic risk factors reliable predictors? *Am. J. Obstet. Gynecol.* **192**, 1933–1935, discussion 1935–1938 (2005).
33. R. B. Gherman *et al.*, Shoulder dystocia: The unpreventable obstetric emergency with empiric management guidelines. *Am. J. Obstet. Gynecol.* **195**, 657–672 (2006).
34. J. Bérard *et al.*, Fetal macrosomia: Risk factors and outcome. A study of the outcome concerning 100 cases >4500 g. *Eur. J. Obstet. Gynecol. Reprod. Biol.* **77**, 51–59 (1998).
35. H. Ju, Y. Chadha, T. Donovan, P. O'Rourke, Fetal macrosomia and pregnancy outcomes. *Aust. N. Z. J. Obstet. Gynaecol.* **49**, 504–509 (2009).
36. H. U. Ezegwui, L. C. Ikeako, C. Egbuji, Fetal macrosomia: Obstetric outcome of 311 cases in UNTH, Enugu, Nigeria. *Niger. J. Clin. Pract.* **14**, 322–326 (2011).
37. H. Vidarsdottir, R. T. Geirsson, H. Hardardottir, U. Valdimarsdottir, A. Dagbjartsson, Obstetric and neonatal risks among extremely macrosomic babies and their mothers. *Am. J. Obstet. Gynecol.* **204**, 423.e1–423.e6 (2011).
38. I. Sjöberg, K. Erichs, I. Bjerre, Cause and effect of obstetric (neonatal) brachial plexus palsy. *Acta Paediatr. Scand.* **77**, 357–364 (1988).
39. T. L. Gross, R. J. Sokol, T. Williams, K. Thompson, Shoulder dystocia: A fetal-physician risk. *Am. J. Obstet. Gynecol.* **156**, 1408–1418 (1987).
40. H. F. Sandmire, T. J. O'Halloin, Shoulder dystocia: Its incidence and associated risk factors. *Int. J. Gynaecol. Obstet.* **26**, 65–73 (1988).
41. N. K. Dajani, E. F. Magann, Complications of shoulder dystocia. *Semin. Perinatol.* **38**, 201–204 (2014).
42. W. R. Trevathan, Fetal emergence patterns in evolutionary perspective. *Am. Anthropol.* **90**, 674–681 (1988).
43. R. B. Gherman *et al.*, Shoulder dystocia: The unpreventable obstetric emergency with empiric management guidelines. *Am. J. Obstet. Gynecol.*, **195**, 657–672 (2006).
44. I. G. Fazekas, F. Kosà, E. Kerner, *Forensic Fetal Osteology* (Akadémiai Kiadó, Budapest, Hungary, 1978).
45. S. Yarkoni, W. Schmidt, P. Jeanty, E. A. Reece, J. C. Hobbins, Clavicular measurement: A new biometric parameter for fetal evaluation. *J. Ultrasound Med.* **4**, 467–470 (1985).
46. S. Black, L. Scheuer, Age changes in the clavicle: From the early neonatal period to skeletal maturity. *Int. J. Osteoarchaeol.* **6**, 425–434 (1996).
47. D. M. Sherer *et al.*, Fetal clavicle length throughout gestation: A nomogram. *Ultrasound Obstet. Gynecol.* **27**, 306–310 (2006).
48. K. Feld, M. Bonni, F. Körber, F. Eifinger, S. Banaschak, Post-mortem estimation of gestational age and maturation of new-borns by CT examination of clavicle length, femoral length and femoral bone nuclei. *Forensic Sci. Int.* **314**, 110391 (2020).
49. J. M. DeSilva, A shift toward birthing relatively large infants early in human evolution. *Proc. Natl. Acad. Sci. U.S.A.* **108**, 1022–1027 (2011).
50. M. Kagaya, N. Ogihara, M. Nakatsukasa, Is the clavicle of apes long? An investigation of clavicular length in relation to body mass and upper thoracic width. *Int. J. Primatol.* **31**, 209–217 (2010).
51. W. Trevathan, K. Rosenberg, The shoulders follow the head: Postcranial constraints on human childbirth. *J. Hum. Evol.* **39**, 583–586 (2000).
52. E. R. Agosto, B. M. Auerbach, Evolvability and constraint in the primate basicranium, shoulder, and hip and the importance of multi-trait evolution. *Evol. Biol.* **48**, 221–232 (2021).
53. M. W. Grabowski, J. D. Polk, C. C. Roseman, Divergent patterns of integration and reduced constraint in the human hip and the origins of bipedalism. *Evolution* **65**, 1336–1356 (2011).
54. M. Grabowski, C. C. Roseman, Complex and changing patterns of natural selection explain the evolution of the human hip. *J. Hum. Evol.* **85**, 94–110 (2015).
55. N. M. Young, G. P. Wagner, B. Hallgrímsson, Development and the evolvability of human limbs. *Proc. Natl. Acad. Sci. U.S.A.* **107**, 3400–3405 (2010).
56. A. M. Mallard, K. R. R. Savell, B. M. Auerbach, Morphological integration of the human pelvis with respect to age and sex. *Anat. Rec. (Hoboken)* **300**, 666–674 (2017).
57. D. M. Bramble, D. E. Lieberman, Endurance running and the evolution of *Homo*. *Nature* **432**, 345–352 (2004).
58. N. T. Roach, M. Venkadesan, M. J. Rainbow, D. E. Lieberman, Elastic energy storage in the shoulder and the evolution of high-speed throwing in *Homo*. *Nature* **498**, 483–486 (2013).
59. R. M. J. Campbell Jr. *et al.*, The characteristics of thoracic insufficiency syndrome associated with fused ribs and congenital scoliosis. *J. Bone Joint Surg. Am.* **85**, 399–408 (2003).
60. J. M. DeSilva, N. M. Laudicina, K. R. Rosenberg, W. R. Trevathan, Neonatal shoulder width suggests a semirotational, oblique birth mechanism in *Australopithecus afarensis*. *Anat. Rec. (Hoboken)* **300**, 890–899 (2017).
61. R. L. Holloway, D. C. Broadfield, K. J. Carlson, New high-resolution computed tomography data of the Taung partial cranium and endocast and their bearing on metopism and hominin brain evolution. *Proc. Natl. Acad. Sci. U.S.A.* **111**, 13022–13027 (2014).
62. T. Sakai *et al.*, Fetal brain development in chimpanzees versus humans. *Curr. Biol.* **22**, R791–R792 (2012).
63. A. C. Halley, Minimal variation in eutherian brain growth rates during fetal neurogenesis. *Proc. Biol. Sci.* **284**, 20170219 (2017).
64. Y. Yamaguchi, S. Yamada, The Kyoto Collection of Human Embryos and Fetuses: History and recent advancements in modern methods. *Cells Tissues Organs* **205**, 314–319 (2018).
65. B. J. Anson, T. H. Bast, S. F. Richany, The fetal and early postnatal development of the tympanic ring and related structures in man. *Ann. Otol. Rhinol. Laryngol.* **64**, 802–823 (1955).
66. B. H. Smith, T. L. Crummett, K. L. Brandt, Ages of eruption of primate teeth: A compendium for aging individuals and comparing life histories. *Am. J. Phys. Anthropol.* **37**, 177–231 (1994).
67. M. F. Ashley-Montagu, The medio-frontal suture and the problem of metopism in the primates. *J. R. Anthropol. Inst. Great Brit. Ireland* **67**, 157–201 (1937).
68. W. M. Krogman, Studies in growth changes in the skull and face of anthropoids. II. Ectocranial and endocranial suture closure in anthropoids and Old World apes. *Am. J. Anat.* **46**, 315–353 (1930).